JOURNAL OF PHYSICAL ORGANIC CHEMISTRY
J. Phys. Org. Chem. 2005; **18:** 298–309
Published online 7 September 2004 in Wiley InterScience (www.interscience.wiley.com). DOI: 10.1002/poc.846

Dimerization mechanisms of heterocyclic carbenes

David C. Graham,[1] Kingsley J. Cavell[2] and Brian F. Yates[1]*

[1]School of Chemistry, University of Tasmania, Private Bag 75, Hobart, Tasmania 7001, Australia
[2]Chemistry Department, Cardiff University, Park Place, Cardiff CF10 3TB, UK

Received 12 May 2004; accepted 1 June 2004

ABSTRACT: The dimerization reactions of a series of heterocyclic carbenes based on the 1,3-dimethylimidazol-2-ylidene template were studied extensively using molecular orbital calculations. The carbenes studied were the 1,3-XY five-membered ring heterocyclic carbenes with all 10 possible combinations of X,Y = NCH_3, PCH_3, O and S. Two different mechanisms for dimerization were studied: a direct carbene plus carbene dimerization reaction and a proton-catalysed dimerization. The parent carbene with XY = NN is found to be kinetically and thermodynamically stable under both mechanisms, whereas XY = NS is predicted to be kinetically stable under aprotic conditions. All remaining carbenes were predicted to be not particularly stable towards dimerization. Indirect schemes for calculating the stability of carbenes towards dimerization were found to give good estimates of the enthalpy of dimerization, but do not take into account the activation barriers. Copyright © 2004 John Wiley & Sons, Ltd.
Supplementary electronic material for this paper is available in Wiley Interscience at http://www.interscience.wiley.com/jpages/0894-3230/suppmat/

KEYWORDS: heterocyclic carbenes; dimerization; DFT calculations

INTRODUCTION

The problems associated with the isolation of free *N*-heterocyclic carbenes were evident as early as the 1960s when attempts were made by Wanzlick and Schikora to isolate 1,3-diphenylimidazolin-2-ylidene. Although the existence of the carbene was proposed via trapping experiments, repeated attempts to isolate the stable free carbene afforded the corresponding dimer as a result of the carbene's intrinsic high reactivity (Scheme 1).[1]

Resurgence in the heterocyclic carbene field sparked by Arduengo *et al.*'s successful isolation of 1,3-diadamantylimidazol-2-ylidene[2] led to the synthesis of a number of carbenes stabilized by adjacent heteroatoms other than nitrogen (Fig. 1).[3–5] These 'second-generation' carbenes appear less thermodynamically stable when compared with the imidazol-2-ylidenes and therefore seem more prone to dimerization. This problem has been overcome by sequestering the carbenic centre with steric bulk in order to provide sufficient kinetic stability for isolation, a method which has allowed the successful isolation of acyclic diamino-, aminoxy- and oxythiocarbenes and also imidazolin-2-ylidenes and thiazol-2-ylidenes.[3,4,6] Only through appropriate protection, it seems, can carbene systems other than diamino be isolated as 'bottle-able' species.

The thermodynamic susceptibility of *N*-heterocyclic carbenes with regard to a number of simple intra- and intermolecular substitution reactions has been comprehensively studied using theoretical methods and dimerization found to be the most common factor preventing the isolation of free carbenes.[6–8] The alternative 1,2-methyl shifts,[8] 1,2-hydrogen-shifts[8,9] and alkyl CH insertion[10] have been found to be less thermodynamically or kinetically favourable compared with dimerization.

Investigations attempting to establish the active catalytic species in the benzoin condensation led to three proposed pathways for carbene dimerization.[11–17] The direct dimerization and indirect proton-catalysed dimerization (via addition or insertion) are illustrated in Scheme 2.

Direct carbene dimerization [Scheme 2 (i)] is regarded as the most common mechanism for formation of the dimer (see below). Chen and Jordan[16] demonstrated via NMR crossover experiments with thiazolium salts the existence of an unsymmetric protonated dimer (**5**, X = NMe, Y = S) that supported the addition mechanism of the proton-catalysed dimerization pathway [Scheme 2 (iib)]. Reinforcing the likelihood of an alternative to direct carbene dimerization, Arduengo *et al.*[3] noted that dimerization of their bottle-able 3-diisopropylphenyl-4,5-dimethylthiazol-2-ylidene proceeded smoothly in the presence of trace amounts of protic acids, whereas under aprotic conditions dimeric products could not be detected on a time-scale of weeks. Further evidence for rate changes of dimerization reactions in the presence of protons is also available for diaminocarbenes.[18]

This is not to say that *N*-heterocyclic carbenes will not dimerize in the absence of protons; in fact, equilibria between benzoimidazol-2-ylidene and its corresponding dimer (**6**) (Fig. 2) have been observed experimentally under conditions that meticulously exclude proton

**Correspondence to:* B. F. Yates, School of Chemistry, University of Tasmania, Private Bag 75, Hobart, Tasmania 7001, Australia.
E-mail: brian.yates@utas.edu.au
Contract/grant sponsor: Australian Research Council (ARC).

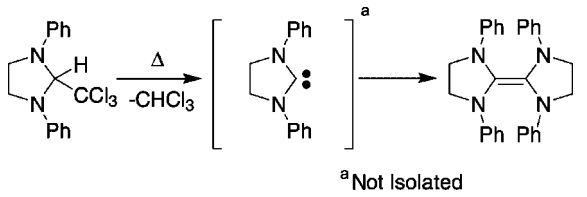

Scheme 1. Wanzlick's and Schikora attempted carbene isolation

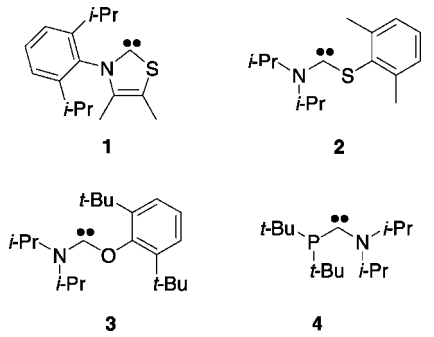

Figure 1. Isolated carbenes showing diversity from diamino substitution

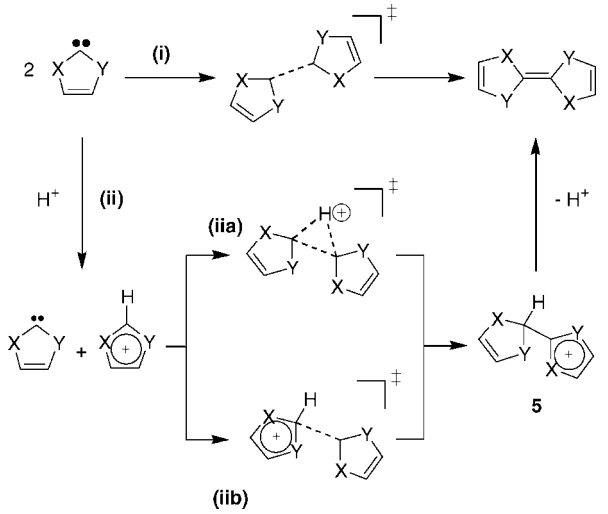

Scheme 2. Dimerization pathways for free carbenes: (i) direct carbene + carbene dimerization; (ii) proton-catalysed dimerization [(iia) insertion mechanism and (iib) addition mechanism]

impurities.[19] No evidence for dimerization has been observed for imidazol-2-ylidenes with the strength of the internal C═C bond shown to be extremely weak, even when the carbene units are constrained together via a tether (**7**).[20]

Despite evidence that thiazol-2-ylidenes decompose via a proton-catalysed mechanism and subsequent information implying acid catalysis of some diaminocarbene dimerizations, recent theoretical studies[7,8,21,22] have ignored this alternative pathway, opting only to study the direct carbene dimerization route. Theoretical work on

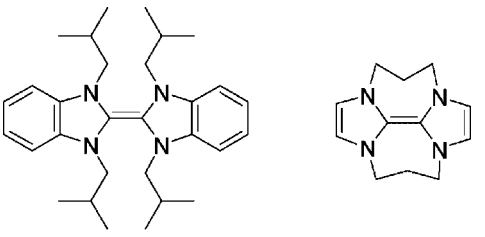

Figure 2. Experimentally observed carbene dimers

direct carbene dimerization has attempted to correlate various factors with the enthalpy of reaction. Singlet–triplet splittings,[7] isodesmic reaction schemes[23,24] and aromaticity[7,8] have all shown a degree of correlation to both the ΔH and E_{act} of dimerization. The absence of a significant kinetic barrier to dimerization or a barrier in accordance with Hammond's postulate[25] is usually assumed.

In general, studies on heterocylic carbenes where proton-catalysed dimerization is explored as an alternative to direct carbene dimerization have been lacking.[8] Theoretical work based on simple acyclic diaminocarbenes has referred to the possible involvement of protons in dimerization,[21] but there is no theoretical work at present detailing proton-catalysed dimerization of cyclic heterocyclic carbenes. Cheng and Hu[7] performed the only complete theoretical investigation of the direct dimerization of imidazol-2-ylidene, reporting a barrier of 19.4 kcal mol^{-1} (1 kcal = 4.184 kJ) and a reaction enthalpy of +1.1 kcal mol^{-1}. Nyulászi's group[23] have investigated the dimerization of thiazol-2-ylidene and dithiol-2-ylidene using theoretical methods, although no activation barriers were calculated.

Here the susceptibility of a series of five-membered unsaturated heterocyclic carbenes to direct dimerization was investigated [Fig. 3 (**CB**)]. The neighbouring atoms were chosen as they are akin to those that have recently been identified as stable species (Fig. 1). Additionally, the reactivity of a subset of these carbenes (X,Y = N, S and O) was analysed with respect to proton-catalysed dimerization and the results are compared with the direct route.

An assessment of the barriers and enthalpies of dimerization via the two mechanisms was carried out using density functional theory (DFT). Furthermore, the applicability of indirect methods utilized in the recent literature to estimate the susceptibility to dimerization was assessed, with mixed results.

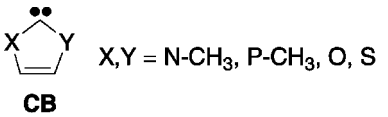

Figure 3. The set of heterocyclic carbenes studied

COMPUTATIONAL METHODS

All geometry optimizations were carried out at the B3LYP[26–28] density functional level of theory employing a 6–31G(d)[29] basis set. High-level energy calculations on these optimized geometries were carried out at the B3LYP level using a 6–311+G(2d,p)[30–32] basis set and include unscaled zero point vibrational energy (ZPVE) corrections from frequency calculations at the lower level of theory (giving ΔH_0). Energies are discussed at the B3LYP/6–311+G(2d,p)//B3LYP/6–31G(d)+ZPVE level unless noted otherwise. Activation barriers (E_{act}) are given as the difference between the energies of the transition structure and precursor complex ($E_{ts} - E_{pc}$). Singlet–triplet splittings were calculated using coupled cluster methods[33,34] at the CCSD(T)/6–311G(d,p)//B3LYP/6–31G(d)+ZPVE level using optimized geometries for both the singlet and triplet species. $<S^2>$ values for all the triplet species were acceptable, with the highest value being 2.13 for the carbene containing P and S.

The nature of the stationary points was determined by evaluating the Hessian matrix. All calculations were carried out with the Gaussian 98 suite of programs.[35]

RESULTS AND DISCUSSION

Direct carbene dimerization

Geometries. The calculated geometries of the 10 singlet carbenes (**CB**, X,Y = NCH_3, PCH_3, O and S) are shown in Fig. 4. A subset of the molecules has been published previously at both the MNDO[36] and MP2[37] levels, and the results shown here are in satisfactory agreement with the previously calculated geometries. Experimental structures are available for **NN** and **NS**

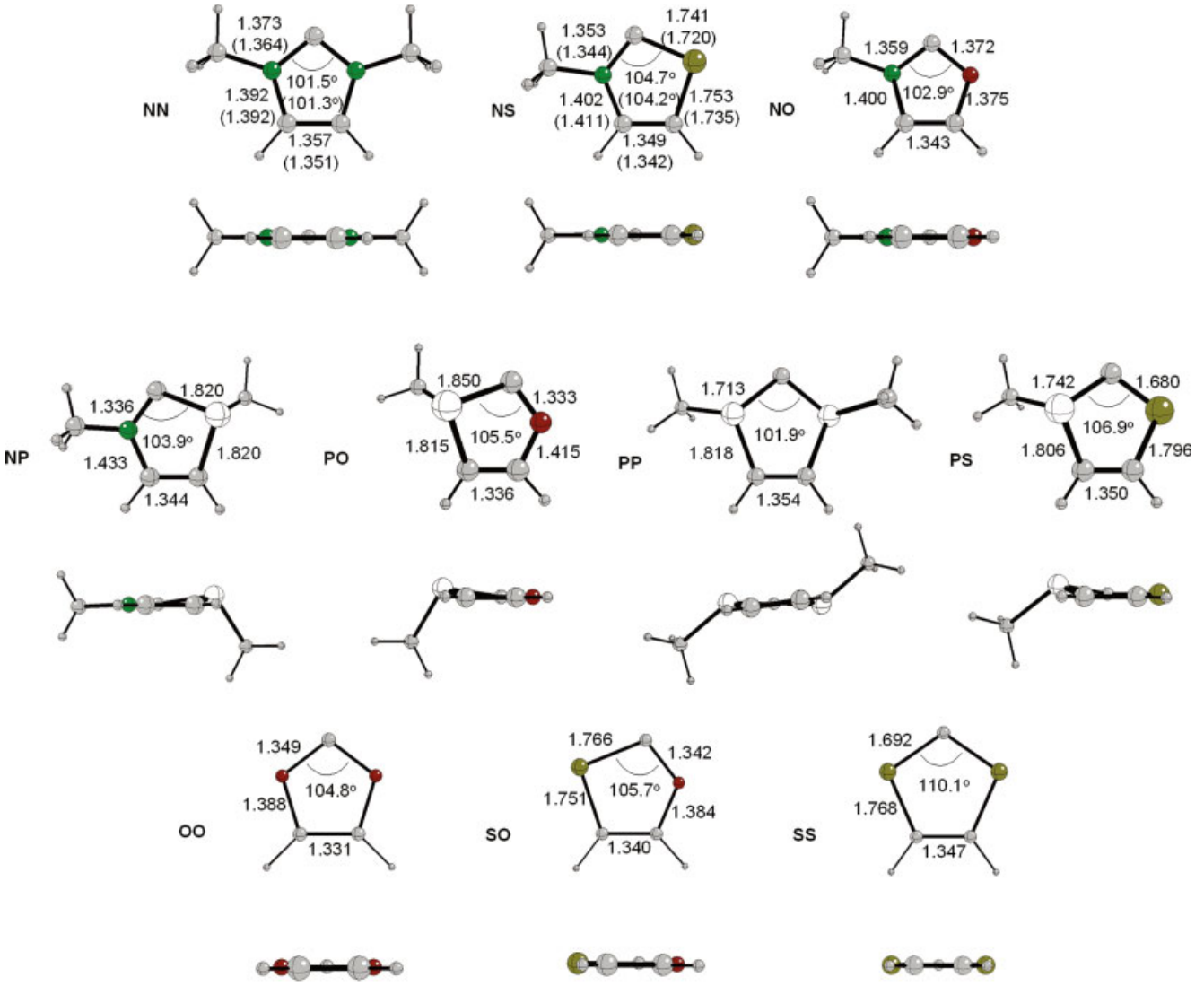

Figure 4. Optimized singlet geometries of the **XY** heterocyclic carbenes (**CB**). Each molecule is shown from two perspectives (top and end-on). Numbers shown in parentheses correspond to experimental structures: 1,3,4,5-tetramethylimidazol-2-ylidene[38] and 3-diisopropylphenyl-4,5-dimethylthiazol-2-ylidene[3]. (This figure is available in colour online)

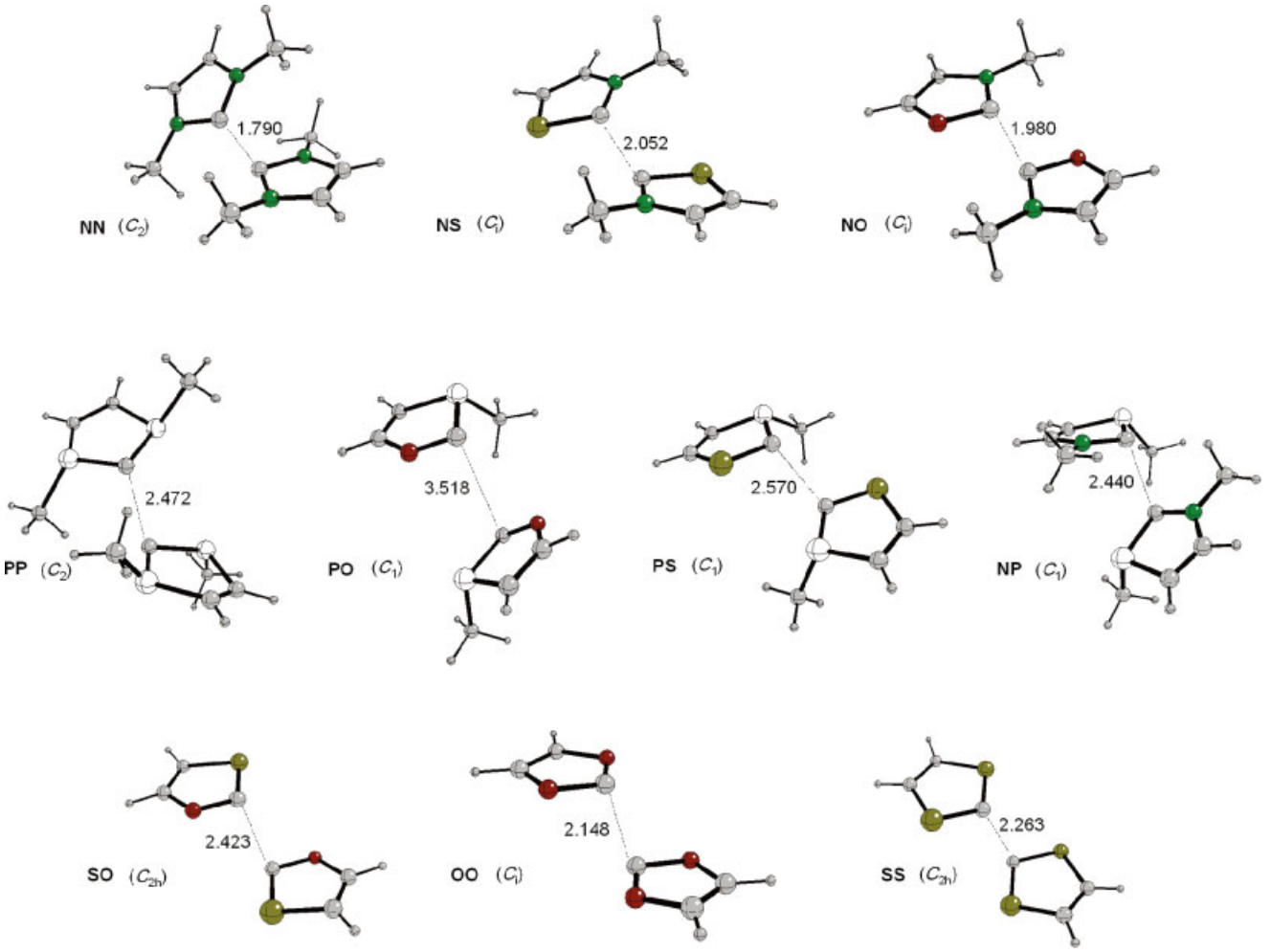

Figure 5. Optimized transition structure geometries and point groups [B3LYP/6–31G(d)] on the direct dimerization pathway (**TS-DD**). (This figure is available in colour online)

carbenes[3,38] and the geometric parameters for the central cores of the heterocycles calculated in the current work are similar to the experimental values (shown in parentheses).

While the majority of the 10 carbenes exhibit a planar five-membered core, those heterocyclic carbenes that contain phosphorus are buckled. Phosphorus prefers a pyramidal conformation in each of the carbenes largely as a result of its high inversion barrier in comparison with nitrogen (PH_3 35 vs NH_3 6 kcal mol^{-1}).[39]

The optimized geometries for the transition structure (**TS-DD**) on the direct carbene dimerization pathway [Scheme 2 (i)] for each of the 10 carbenes is shown in Fig. 5.

The transition structure geometries all support the non-least motion pathway approach of the two carbenes, where the repulsion of lone pairs implicit in the least motion (direct) approach is avoided and replaced by a bonding electrophilic–nucleophilic interaction (Fig. 6).[40] The non-least motion pathway also eliminates steric interaction that would occur between exocyclic ring substituents (i.e. methyl groups) inherent in the least motion approach. Arduengo *et al*. have modeled the dimerization of unsaturated *N*-heterocyclic carbenes via the reaction of 1,3-bis(2,4,6-trimethylphenyl)imidazol-2-ylidene with GeI_2 and x-ray structural analysis of the resulting adduct lends support to the non-least motion pathway for singlet carbene dimerization.[41]

Approach of the two carbenes is not strictly perpendicular to the plane of the carbenes. Whereas OO, SS and SO do exhibit this high degree of symmetry (C_{2h}, C_{2h} and C_i, respectively), the other transition structures show one carbene attacking the other with a more side-on approach

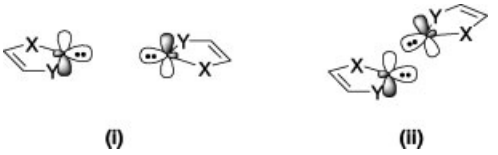

Figure 6. Carbene approach methods: (i) least motion; (ii) non-least motion

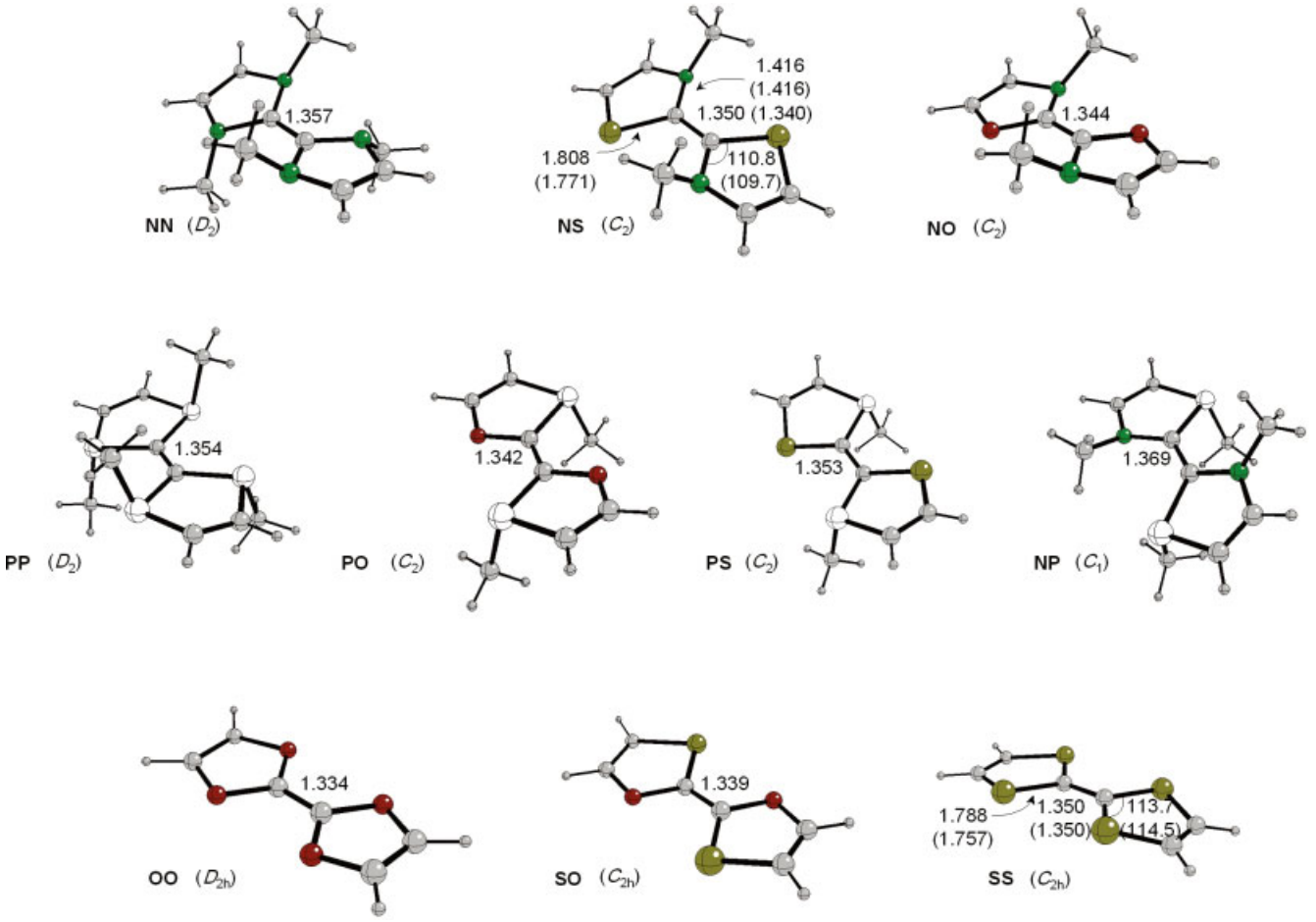

Figure 7. Optimized dimer geometries and point groups [B3LYP/6–31G(d)] (**PRD**). Numbers shown in parentheses correspond to the average measurements in the experimental structures: bis(3,4,5-trimethylthiazol-2-ylidene)[3] and tetrathiafulvalene[42]. (This figure is available in colour online)

in order to minimize steric repulsion between the exocyclic ring substituents.

The C(2)—C′(2) bond lengths in the transition structures vary in the range 1.79–3.52 Å. The cause of this is likely to be predominantly electronic in nature, as those heterocycles with minimal steric bulk (i.e. **OO**, **SO** and **SS**) exhibit considerably longer bond lengths than the sterically crowded **NN** transition structure. Alternate transition structures for the **PO**, **PS** and **NP** carbenes were located in which the methyl groups occupy different positions (see Supplementary Material). The **PO**- and **NP**-based structures contained two imaginary frequencies unrelated to the dimerization reaction vector. One of the additional **PS** transition structures located, while lower in energy than that shown in Fig. 5, led to a less stable dimer conformer on following the reaction vector toward the product (see below).

The geometries of the dimer products are shown in Fig. 7. In the cases where similar experimental structures are available, the comparative geometric data are given in parentheses. Calculated geometries are in good agreement with the experimental data, but it should be noted that the conformation of the experimental structure for the **NS** dimer differs significantly from the calculated conformer (Fig. 8, **I**). This thiazole-based dimer, obtained by Arduengo *et al.*[3] on dimerization of two carbene units, is unsymmetrical in comparison with the **NS** dimer shown in Fig. 7, with only one of the two nitrogen atoms exhibiting sp^3 hybridization. Strangely, this experimental structure was easily located at B3LYP/6–31G(d) after substitution of the backbone hydrogens (in **NS**-**PRD**) for methyl groups (**II**). Hence it appears that there is a strong structural dependence of the conformation of the **NS** dimer on even the simplest backbone substitution. An additional C_2 symmetric **NS** dimer with methyl groups on

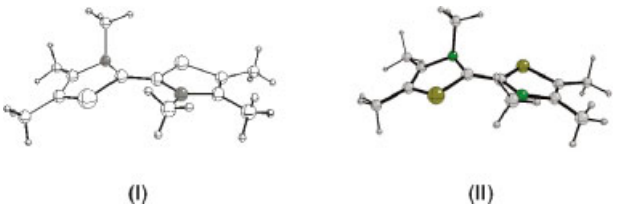

Figure 8. Experimental crystal structure for the **NS** dimer [bis(3,4,5-trimethylthiazol-2-ylidene)] (**I**)[3] and the corresponding C_1 minima located on the B3LYP/6–31G(d) PES (**II**). (This figure is available in colour online)

the backbone similar to that shown in Fig. 7 was also found lying 0.46 kcal mol^{-1} below structure **II**, hence crystal packing effects may also play a small role in stabilizing the experimental structure **I**.

The dimer geometries all exhibit comparable C(2)—C′(2) bond lengths of 1.35 ± 0.02 Å. Any deviation that does exist in the bond lengths appears to be attributed to steric strain, with those carbene units bearing two exocyclic ring substituents (**NN**, **NP** and **PP**) having elongated C—C bonds in comparison with those bearing one or no exocyclic substituents. Nitrogen and phosphorus both prefer to adopt non-planar (sp^3) orientations, as has been shown both experimentally[3] and theoretically[9] for similar systems. Presumably this effect occurs in an attempt to reduce steric repulsion between the nitrogen and phosphorus exocyclic ring substituents.

In the cases where more than one geometric isomer of the dimer could exist, calculations were performed on all isomers to ascertain the lowest energy conformer. The lowest energy isomers that were found all adopt similar geometries, with the heteroatoms in opposing carbene units *trans* to one another, R groups *trans* in the same carbene unit and R groups *cis* on the same heteroatom across carbene units (Fig. 9). Experimentally isolable saturated analogues for both **NN** and **PP** dimers also exhibit this exact conformation.[43–45]

All additional modelled conformations exhibited zero imaginary frequencies implying true minima, whereas dimers of other conformations exhibited one or more imaginary frequencies, were higher in energy, or both. The geometric data for the higher energy conformations can be found in the Supplementary Material.

Direct dimerization potential energy surface. The energies for the structures on the direct carbene dimerization pathway [Scheme 2 (i)] are given in Table 1 and expressed graphically in Fig. 10. The initial contact between the two free carbene units results in a precursor complex that is more stable than the separated reactants at the optimization level of theory; however, single point calculations at the higher level raise the energy of the precursor complexes slightly above that of the reactants when XY = **OO**, **SO** and **SS**.

The dimerization of nine of the 10 **XY** carbenes is exothermic although, based on previous ΔH and ΔG calculations, entropy considerations are expected to disfavour dimerization by an additional 10 kcal mol^{-1}.[8,23] The dimerization enthalpy of the **NN** carbene is approximately thermoneutral at -0.7 kcal mol^{-1}, a result which

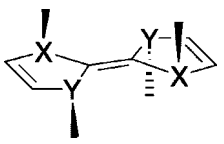

Figure 9. Conformation of the lowest energy dimer (X,Y = NMe, O, S and PMe)

Table 1. Relative energies on pathway (i)[a] (direct dimerization)

Carbene	Reactants (**RCT-DD**)	Precursor complex (**PC-DD**)	Transition structure (**TS-DD**)	Dimer product (**PRD**)
NN	0.0	−0.8	22.6	−0.7
NO	0.0	−3.1	9.1	−19.8
NP	0.0	−0.4	3.8	−67.0
NS	0.0	−1.3	13.7	−25.7
OO	0.0	0.3	3.2	−32.5
PO	0.0	−2.7	−1.1	−105.8
PP	0.0	−2.1	8.3	−97.0
PS	0.0	−2.7	5.0	−82.4
SO	0.0	1.0	2.4	−55.4
SS	0.0	0.4	9.4	−48.3

[a] All values are in kcal mol^{-1} and are relative to reactants.

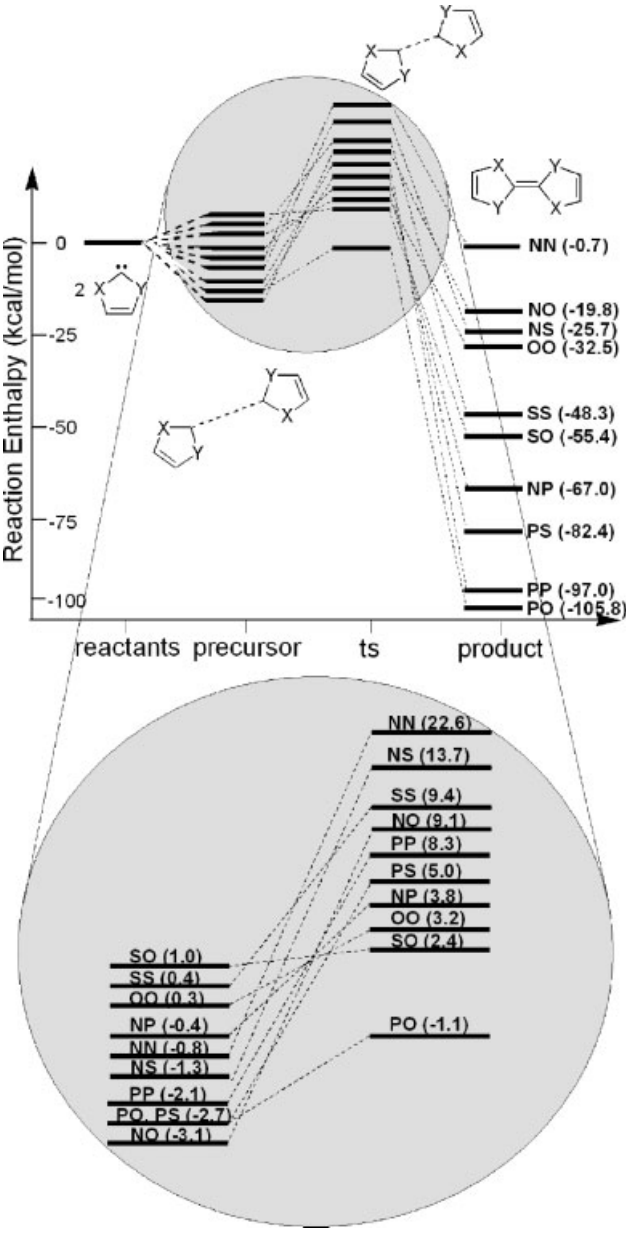

Figure 10. Graphical representation of the direct carbene dimerization potential energy surface (i)

Table 2. Various properties of heterocyclic carbenes (kcal mol^{-1})

Carbene	E_{act} (dimerization)	ΔH (dimerization)	ΔH (**R1**)[a]	*BDE* (**R2**)[b]	ΔE_{s-t}[c]
NN	23.4	−0.7	106.0	4.6	83.7
NO	12.2	−19.8	96.5	12.5	79.8
NP	4.2	−67.0	72.5	99.3	36.3
NS	15.0	−25.7	94.1	36.4	67.8
OO	2.8	−32.5	86.1	18.5	76.7
PO	1.6	−105.8	53.0	119.4	26.3
PP	10.4	−97.0	53.5	134.3	18.8
PS	7.7	−82.4	63.0	111.2	30.4
SO	1.4	−55.4	78.8	57.7	57.1
SS	9.0	−48.3	82.6	66.9	52.6

[a] Nyulászi *et al.*'s isodesmic reaction enthalpy (**R1**).[23]
[b] Bond dissociation energy (**R2**).[24]
[c] Singlet–triplet splitting ($\Delta E_{s-t} = E_{triplet} - E_{singlet}$).

parallels findings using estimates obtained from both direct[7,8] and indirect[9,23] computational methods. The **NN**, **NO**, **NS** and **OO** carbenes are thermodynamically more stable to dimerization than the remainder of the carbene set, with reaction enthalpies more positive than −32.5 kcal mol^{-1}. The phosphorus-containing carbenes exhibit the greatest thermodynamic driving force to dimerization via the direct route, with their instability likely to be associated with their expected lack of aromatic character as a result of sp^3 hybridization of phosphorus in the free carbene. The large enthalpies of dimerization exhibited by these less aromatic carbenes agree with a number of reports that correlate ΔH(dimerization) with aromaticity.[7–9,23,46,47]

The activation energies for dimerization (E_{act}) range from almost non-existent (for **SO** and **PO**) to an appreciable 23.4 kcal mol^{-1} for **NN** (Table 2).

Recent studies comparing imidazol-2-ylidenes with the less aromatic imidazolin-2-ylidenes have supported the argument that, in addition to thermodynamic stability of the product, high barriers to dimerization are also associated with the aromatic character of the carbene.[7,8] Increased aromaticity is associated with the increased donation from adjacent groups into the formally empty p_π orbital, which reduces the electrophilic nature of the carbene, a critical component in the dimerization pathway.[46,48] While in general this same trend is evident here with the **NP**, **PO** and **PS** carbenes exhibiting low barriers to dimerization, it fails to hold for the **PP** pathway, which is non-aromatic but has an appreciable E_{act} of 10.2 kcal mol^{-1}. This discrepancy may be attributed to the increased steric bulk in the transition structure associated with the four exocyclic methyl groups.

Estimating the tendency to dimerize via indirect methods. The enthalpy of dimerization for heterocyclic carbenes is available through a number of indirect methods that avoid the overhead of large calculations on the entire system. The isodesmic reaction scheme used by Nyulászi *et al.*[23] (Scheme 3, **R1**) and the bond dissociation energy[24] (BDE) (Scheme 3, **R2**), which is based on the carbene singlet–triplet splitting, both show excellent correlation with the enthalpy of dimerization with R^2 values of 0.99 and 0.93 respectively (Table 2 and Fig. 11). This relationship demonstrates that these indirect methods are useful in estimating the enthalpy of dimerization for the series of heterocyclic carbenes studied in this work.

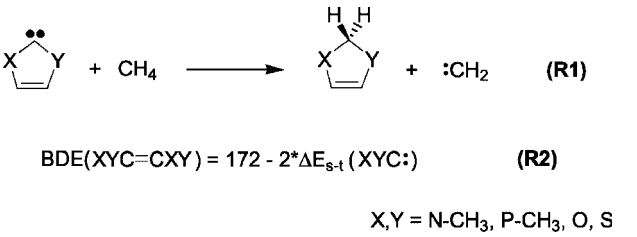

Scheme 3. Reaction schemes for indirect determination of dimerization susceptibility

Despite this pleasing result, the likelihood of free carbene dimerization cannot be assessed based on the enthalpy of the reaction alone. The barrier to dimerization (E_{act}) must also be taken into account when determining the likelihood of carbene dimerization, but the indirect methods surveyed here fail to do this, instead relying on Hammond's postulate to estimate the barrier, assumed to be inversely proportional to the reaction enthalpy. Lack of correlation between ΔH and E_{act} for the dimerization reactions (Fig. 12) shows that the assumption of kinetic stability of carbenes based purely on their thermodynamic stability to dimerization is not always appropriate.

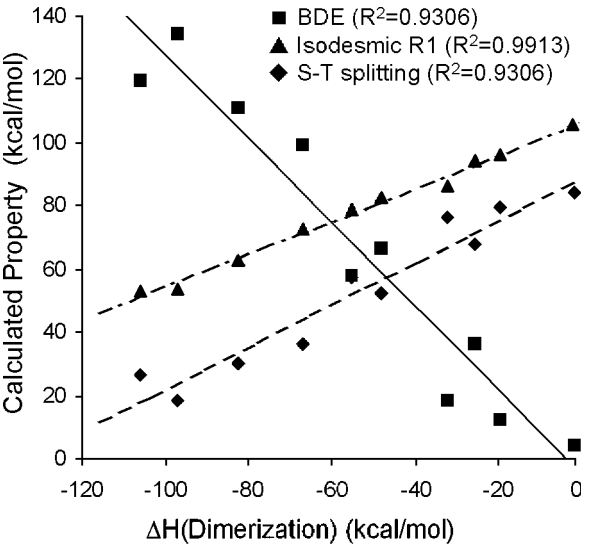

Figure 11. Correlation of *BDE*, ΔH(**R1**) and ΔE_{s-t} with enthalpy of dimerization

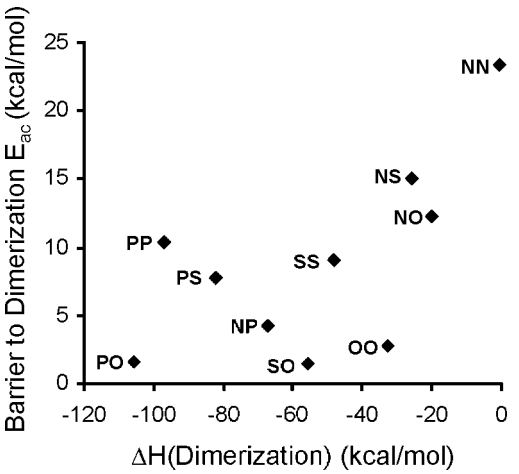

Figure 12. Non-adherence to Hammond's postulate

In accordance with Hammond's postulate,[25] **NN**, **NO** and **NS** carbenes exhibit late transition states, small enthalpies of reaction and high barriers to dimerization (23.4, 12.2 and 15.0 kcal mol^{-1}, respectively). Despite this, the relation between E_{act} and ΔH is not strictly adhered to across the entire series of carbenes investigated. This is not unexpected given that the steric bulk across the series of carbenes varies markedly as we move from the unsubstituted (**OO**, **SO** and **SS**) to monosubstituted (**NS**, **NO**, **PS** and **PO**) and disubstituted (**PP**, **NP** and **NN**) carbenes. A case in point is dioxol-2-ylidene (**OO**), which shows excellent thermodynamic stability but only a small barrier to dimerization (2.8 kcal mol^{-1}), presumably owing in part to the lack of steric protection of the carbene carbon. Large changes in the sterics of the carbene[7] along with significantly dissimilar transition states[49] have previously resulted in a non-conformity of Hammond's postulate for carbene dimerization reactions. Prior studies where ΔH and E_{act} *have* shown good correlation typically have very little variation of the structures considered.[7,8] In fact, Cheng and Hu[7] only achieved good correlation between ΔH and E_{act} after outliers that contained considerable bulk were excluded from the sample set.

In summary, although ΔH(dimerization) can be estimated reasonably well based on the properties of the carbene itself (i.e. ΔE_{s-t}) and isodesmic reaction schemes, E_{act}(dimerization) appears to be a function of not only the electronic nature of the free carbene but also the steric protection provided by the exocyclic groups, making estimation of this quantity via indirect methods more difficult.

Proton-catalysed dimerization

The alternative dimerization pathway proposed by Metzger *et al.*[11] [Scheme 2 (ii)] contains an intermediate that can be formed through CH insertion [Scheme 2 (iia)] or via nucleophilic attack on the carbene carbon [Scheme 2 (iib)].[16] Despite rigorous searching of the potential energy surfaces, no transition structures for the insertion mechanism could be located for the carbenes studied here. Although insertion of heterocyclic carbenes into acidic CH bonds is commonly observed,[50] the strongly basic nature of the carbene[51] means that formation of the intermediate through CH insertion is unlikely. The conclusion that the intermediate is formed via addition rather than insertion has been reinforced by experimental evidence for thiazol-2-ylidenes and is generally accepted.[16]

As problems associated with the chirality of phosphorus would greatly complicate the potential energy surfaces for these carbenes, and given the thermodynamic instability of the phosphorus-containing heterocyclic carbenes, the alternate dimerization pathway for phosphorus-based carbenes was omitted.

Geometries. The initial step of the proton-catalysed dimerization (PCD) pathway [see Scheme 2 (iib)] involves the protonation of one carbene to form an -olium salt. The initial precursor complexes located on the potential energy surface are formed by a long-distance interaction between the free carbene and the corresponding -olium salt (Fig. 13). These C—H—C type complexes have been isolated experimentally for the **NN** precursor complex,[52] with the experimental x-ray data found to be in excellent agreement with the calculated values. With the exception of the **NO** precursor complex, all the encounter complexes exhibit the same C—H—C

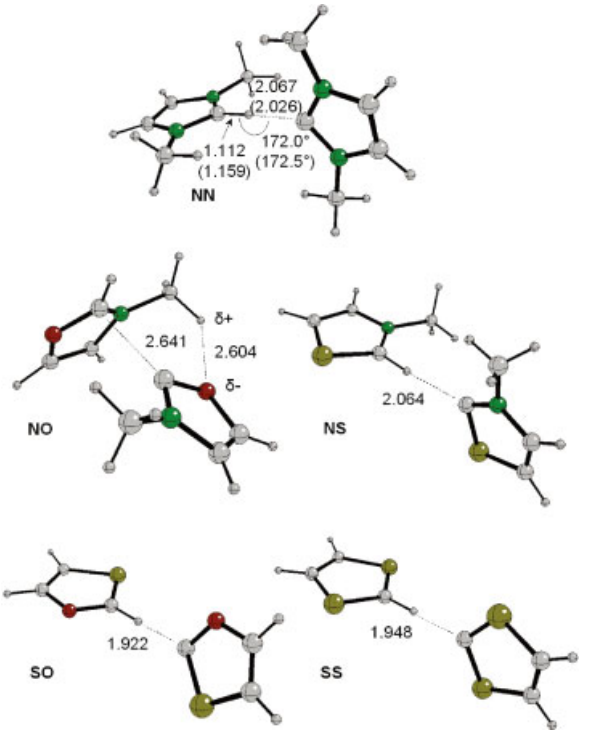

Figure 13. Precursor complexes (**PC-PCD**) on the proton-catalysed dimerization pathway. (This figure is available in colour online)

hydrogen-bond geometry. On scanning from the transition structure toward the reactants on the **NO** potential energy surface, an encounter complex was found that closely resembled the transition structure. It is likely that this low-energy minimum is facilitated by an additional hydrogen-bonding interaction between a proton on the methyl group of the oxazolium salt and the electronegative oxygen in the carbene ring. This additional hydrogen-bonding interaction was not observed in any of the other encounter structures.

The geometries of both the transition structures and intermediates for the proton-catalysed dimerization pathway are shown collectively in Fig. 14. No transition structure for **OO** was found and no barrier between the reactants and the intermediate was revealed in potential energy surface scans.

The transition structure geometries are all similar and are what might be expected from the attack of the carbene lone pair on the formally vacant p_π orbital of the C(2) carbon of the -olium salt. The HC(2)—C′(2) bond lengths in the transition structures range from 1.94 to 2.94 Å. As with the transition structures on the direct dimerization pathway, the difference between these bond lengths is likely to be predominantly electronic in nature, with the sterically crowded **NN** transition structure exhibiting a considerably shorter HC(2)—C′(2) bond length than the unencumbered **SO** and **SS** transition structures. The intermediate geometries clearly indicate that the C(2) carbon of the -olium salt is sp^3-hybridized as a result of the attack by the approaching carbene lone pair, whereas the nitrogen atoms of the salts in the nitrogen-containing intermediates adopt a non-planar sp^3 configuration as a result of disrupted electron delocalization.

Proton-catalysed dimerization potential energy surface. All the carbenes show a thermodynamic tendency to form the protonated dimer intermediate from the carbene and salt (Table 3, Fig. 15). Given the strongly basic nature of heterocyclic carbenes, this proceeds with a large enthalpy of reaction ($\Delta H < -220\,\text{kcal mol}^{-1}$) reinforcing the notion that heterocyclic carbenes are among some of the most powerful neutral Lewis bases known.[53] Based on the C—C bond lengths in the transition structures, the **NN** structure is late in comparison with the others and shows the greatest barrier to forming the intermediate ($E_{act} = +15.9\,\text{kcal mol}^{-1}$), in addition to exhibiting a thermodynamic preference for the precursor over the intermediate ($+4.2\,\text{kcal mol}^{-1}$ when referenced to 'carbene plus salt'). Only **NN** and **NS** ($9.1\,\text{kcal mol}^{-1}$) show a significant barrier to dimerization via the proton-catalysed mechanism.

The considerable thermodynamic stability possessed by the protonated dimer intermediates means that the action of a strong base is required in order to abstract the final proton to form the dimer. Any carbene present may act as the base (Scheme 4), making the requirement of an external base unnecessary in some cases.

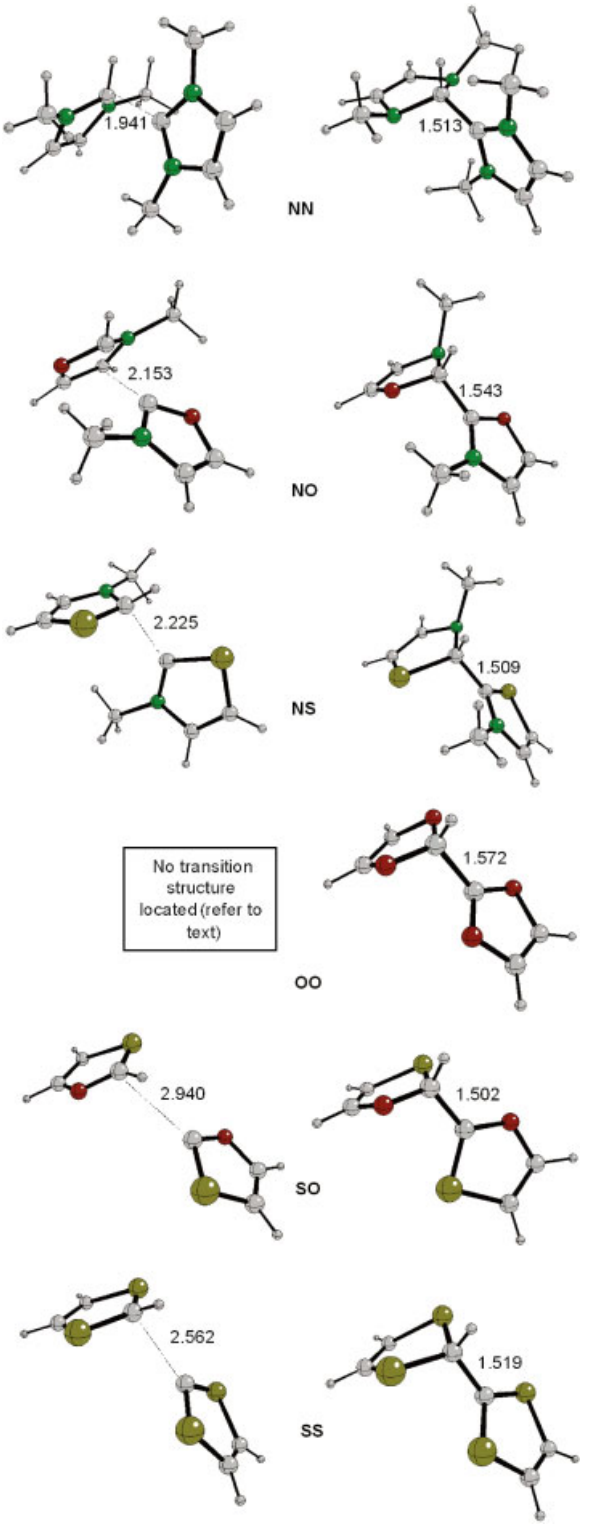

Figure 14. Transition structure (left) (**TS-PCD**) and intermediate geometries (right) (**INT-PCD**) on pathway (iib) Scheme 2. (This figure is available in colour online)

The enthalpy of proton abstraction from the protonated dimer intermediate by the corresponding free carbene is shown in Table 4 (i.e. ΔH for the reaction shown in Scheme 4). In addition to being related to the strength of

Table 3. Relative energies for pathway (iib)[a] (Scheme 2)

Carbene	Reactants	Carbene plus salt	Precursor complex (**PC-PCD**)	TS (rel.)[b] (**TS-PCD**)	Intermediate[b] (**INT-PCD**)	Dimer (**PRD**)
NN	0	−259.5	−275.4	−259.4 (+15.9)	−271.2 (+4.2)	−0.7
NO	0	−243.7	−260.0	−258.2 (+1.8)	−266.9 (−6.9)	−19.8
NS	0	−248.8	−265.1	−256.0 (+9.1)	−272.9 (−7.8)	−25.7
OO	0	−220.9	—	— (−)	−253.6 (−)	−32.5
SO	0	−233.1	−251.2	−248.8 (+2.4)	−274.9 (−23.7)	−55.4
SS	0	−234.9	−250.5	−245.0 (+5.5)	−266.7 (−16.2)	−48.3

[a] Energies are in kcal mol^{-1} and are referenced to the reactants.
[b] Values in parentheses denote the energies relative to the precursor complex.

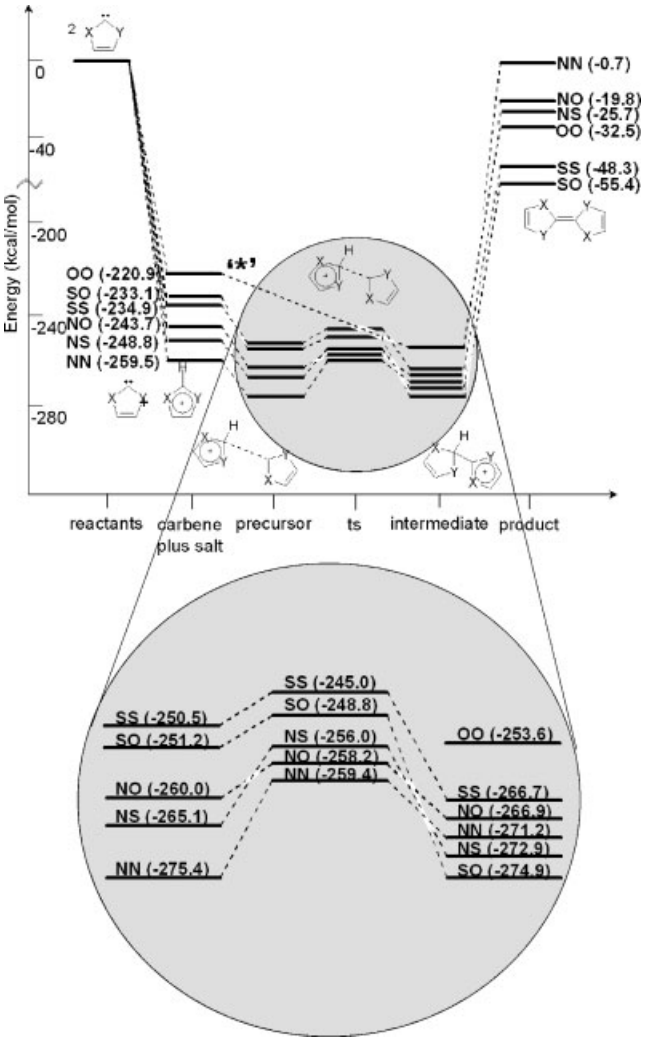

Figure 15. Graphical representation of dimerization energies on pathway (iib), *No transition structure was found for the **OO** pathway (see text)

the C—H bond in the intermediate, this energy is also dependent on the proton affinity of the corresponding carbene. For completeness, the calculated proton affinities for all 10 carbenes studied in this work are provided in the Supplementary Material.

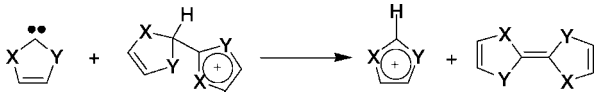

Scheme 4. Deprotonation of the protonated dimer intermediate by its corresponding carbene

Table 4. Enthalpy of proton abstraction from intermediate relative to proton affinity of the carbene (Scheme 4)

Carbene	$\Delta H_{\text{abstraction}}$ (kcal mol^{-1})
NN	10.9
NO	3.3
NS	−1.6
OO	0.1
SO	−13.6
SS	−16.5

The results in Table 4 clearly demonstrate that the **SO** and **SS** intermediates, coupled with their analogous carbenes, have a thermodynamic driving force that prefers the dimer ($\Delta H = -13.6$ and -16.5 kcal mol^{-1}, respectively). Final proton abstraction in the **NN** carbene case is unlikely ($\Delta H = +10.9$ kcal mol^{-1}) and the significant barrier required initially to attain the dimer ($+15.9$ kcal mol^{-1}) would probably prevent the protonated dimer intermediate from being formed. Both of these factors reinforce to make formation of the neutral **NN** dimer unlikely.

Comparison of pathways

The carbenes that show considerable kinetic stability to dimerization via the direct pathway (i.e. **NN**, **NS** and **NO**) all exhibit lower activation energies in the presence of a proton (Table 5).

In the presence of a proton catalyst, the activation energy for dimerization of the **NN** carbene is reduced from $+23.4$ to $+15.9$ kcal mol^{-1}. Nonetheless, these values suggest that **NN** carbenes are kinetically and thermodynamically stable to both dimerization mechanisms. Experimental observations confirm this postulate,

Table 5. Comparison of activation energies for both pathways[a]

Carbene	E_{act}(**DD**)[b]	E_{act}(**PCD**)[c]	$\Delta H_{dimerization}$
NN	23.4	15.9	−0.7
NO	12.2	1.8	−19.8
NP	4.2	—	−67.0
NS	15.0	9.1	−25.7
OO	2.8	0.0[d]	−32.5
PO	1.6	—	−105.8
PP	10.4	—	−97.0
PS	7.7	—	−82.4
SO	1.4	2.4	−55.4
SS	9.0	5.5	−48.3

[a] All energy values are in kcal mol^{-1}.
[b] Free carbene dimerization activation energy [pathway (i)].
[c] Proton-catalysed carbene dimerization [pathway (iib)].
[d] No barrier could be found for this dimerization reaction (see text).

with no recorded observations of dimer formation from free imidazol-2-ylidenes. Indeed, in the presence of hydrogen ions, non-tethered carbenes form a carbene–H–carbene adduct in preference to the dimer.[52]

The presence of protons lowers the activation energy of **NS** dimerization by 5.9 kcal mol^{-1} to +9.1 kcal mol^{-1}. It is possible, then, that otherwise stable **NS** carbenes may form the corresponding dimer in the presence of protons, a phenomenon that has been demonstrated experimentally by Arduengo *et al.*[3]

It is not surprising that heterocyclic **NO** carbenes are yet to be observed, given the low barrier to direct dimerization (12.2 kcal mol^{-1}) and, in particular, to proton-catalysed dimerization (+1.8 kcal mol^{-1}), calculated here. **SS**, **SO** and **OO** carbenes all exhibit a lack of kinetic stability with respect to both dimerization mechanisms and have an increased thermodynamic driving force for dimerization.

It is important to note that experimentally these reactions will probably only occur in a solvent, and the characteristics of this solvent may have a profound effect not only on the barrier to dimerization, but also on which pathway is preferred. Reaction mixtures that rigorously exclude protons will undergo dimerization only via a direct mechanism, if at all. Experimentally, Hahn *et al.* observed this with the dimerization of benzoimidazol-2-ylidenes under conditions where trace Lewis acid impurities are meticulously excluded.[19] In protic solvents or systems where the protonated form of the carbene is available, both direct and proton-catalysed dimerization mechanisms may be possible, with the preferred mechanism likely to be determined by the polarity of the solvent. A preference for proton-catalysed dimerization may occur if the ionic transition structure is stabilized with respect to the reactants—most likely in a highly polar solvent, although exact susceptibilities can be accurately estimated only via computational methods where solvation effects are explicitly calculated.

Steric protection of the carbene centre via the introduction of large exocyclic substituents at nitrogen may increase the kinetic stability of a nitrogen-containing heterocycle. This approach has allowed the successful isolation of a number of carbenes that may otherwise have dimerised.[3,4,6] It is unlikely that we will ever observe **SS**, **SO** and **OO** heterocyclic carbenes owing to the inherent lack of kinetic and thermodynamic stability unless elaborate steric protection for the carbene carbon is incorporated at the 4- and 5-positions of the ring.

CONCLUSIONS

The dimerization pathways for X,Y heterocyclic carbenes have been investigated using density functional theory. Imidazole-based (**NN**) carbenes show thermodynamic stability and a kinetic barrier to dimerization in both of the pathways investigated. Thiazole-based (**NS**) carbenes show stability in aprotic conditions but dimerization becomes more likely in the presence of hydrogen ions. Phosphorus-containing carbenes are predicted to have low barriers to dimerization and have an increased thermodynamic tendency to form the dimer product, probably owing to the sp^3 hybridization of phosphorus in the free carbene preventing aromatic stabilization. Carbenes that lack exocyclic ring substituents (**SO**, **OO** and **SS**) have low barriers to dimerization via both pathways, with **OO** showing no barrier to proton-catalysed dimerization.

In agreement with previous investigations,[16] proton-catalysed dimerization is found to proceed via an addition rather than an insertion mechanism. Whether or not the protonated dimer intermediate is observed experimentally relies on the relative proton affinities of the free carbene and the protonated dimer. Observation of the **SO** and **SS** protonated dimer intermediates is unlikely, given the ease of proton abstraction from the respective protonated dimer by the corresponding free carbene.

The proposed methods for indirectly predicting the dimerization enthalpy extend well across the series of heterocyclic carbenes studied here. Caution must be exercised when suggesting that the kinetic stability of the carbene to dimerization can be assessed using indirect methods such as isodesmic reaction schemes and aromaticity. Owing to steric differences in the range of carbenes considered, the Hammond postulate is not strictly adhered to and as a consequence the barrier to dimerization cannot be adequately estimated.

In polar solvents, both the proton-catalysed and direct dimerization mechanisms may be responsible for producing the final dimer with the preference depending on the nature of the solvent. The ionic nature of the proton-catalysed transition structure is likely to be stabilized in highly polar solvent systems and, in the presence of protons or protonated carbene species (i.e. -olium

salts), a preference for proton catalysed dimerization is expected.

Supplementary material

Computational details for all structures (Cartesian coordinates energies, and the number of imaginary frequencies) and calculated proton affinities for the 10 carbenes studied in this work are available in Wiley Interscience.

Acknowledgements

The authors thank the Australian Research Council (ARC) for project funding and a PhD scholarship for D.C.G. They are also indebted to the Australian Partnership for Advanced Computing (APAC) for a generous time grant on their parallel computing facility.

REFERENCES

1. Wanzlick H-W, Schikora E. *Chem. Ber.* 1961; **94**: 2389–2393.
2. Arduengo AJ, Harlow RL, Kline M. *J. Am. Chem. Soc.* 1991; **113**: 361–363.
3. Arduengo AJ, Goerlich JR, Marshall WJ. *Liebigs Ann.-Recl.* 1997; 365–374.
4. Alder RW, Butts CP, Orpen AG. *J. Am. Chem. Soc.* 1998; **120**: 11526–11527.
5. Merceron N, Miqueu K, Baceiredo A, Bertrand G. *J. Am. Chem. Soc*. 2002; **124**: 6806–6807.
6. Denk MK, Thadani A, Hatano K, Lough AJ. *Angew. Chem. Int. Ed. Engl.* 1997; **36**: 2607–2609.
7. Cheng MJ, Hu CH. *Chem. Phys. Lett.* 2001; **349**: 477–482.
8. Cheng MJ, Hu CH. *Chem. Phys. Lett.* 2000; **322**: 83–90.
9. Heinemann C, Thiel W. *Chem. Phys. Lett.* 1994; **217**: 11–16.
10. Su MD, Chu SY. *Inorg. Chem.* 1999; **38**: 4819–4823.
11. Metzger J, Larive H, Dennilauler R, Baralle R, Gaurat C. *Bull. Soc. Chim. Fr.* 1964; 2857–2867.
12. Castells J, LopezCalahorra F, Geijo F, Perez-Dolz R, Bassedas M. *J. Heterocycl. Chem.* 1986; **23**: 715–720.
13. Chen YT, Barletta GL, Haghjoo K, Cheng JT, Jordan F. *J. Org. Chem.* 1994; **59**: 7714–7722.
14. Bordwell FG, Satish AV. *J. Am. Chem. Soc.* 1991; **113**: 985–990.
15. Castells J, Domingo L, Lopezcalahorra F, Marti J. *Tetrahedron Lett.* 1993; **34**: 517–520.
16. Chen YT, Jordan F. *J. Org. Chem.* 1991; **56**: 5029–5038.
17. LopezCalahorra F, Castro E, Ochoa A, Marti J. *Tetrahedron Lett.* 1996; **37**: 5019–5022.
18. Denk MK, Thadani A, Hatano K, Lough AJ. *Angew. Chem. Int. Ed. Engl.* 1997; **36**: 2607–2609, footnote 19.
19. Hahn FE, Wittenbecher L, Le Van D, Frohlich R. *Angew. Chem. Int. Ed. Engl.* 2000; **39**: 541–544.
20. Taton TA, Chen P. *Angew. Chem. Int. Ed. Engl.* 1996; **35**: 1011–1013.
21. Alder RW, Blake ME, Oliva JM. *J. Phys. Chem. A* 1999; **103**: 11200–11211.
22. Oliva JM. *Chem. Phys. Lett.* 1999; **302**: 35–42.
23. Nyulászi L, Veszpremi T, Forro A. *Phys. Chem. Chem. Phys.* 2000; **2**: 3127–3129.
24. Carter EA, Goddard WA III. *J. Phys. Chem.* 1986; **90**: 998–1001.
25. Hammond GS. *J. Am. Chem. Soc.* 1955; **77**: 334–338.
26. Becke AD. *J. Chem. Phys.* 1993; **98**: 5648–5652.
27. Becke AD. *Phys. Rev. A.* 1988; **38**: 3098–3100.
28. Lee C, Yang W, Parr RG. *Phys. Rev. B* 1988; **37**: 785–789.
29. Hariharan PC, Pople JA. *Theor. Chim. Acta* 1973; **28**: 213–222.
30. Krishnan R, Binkley JS, Seeger R, Pople JA. *J. Chem. Phys.* 1980; **72**: 650–654.
31. McLean AD, Chandler GS. *J. Chem. Phys.* 1980; **72**: 5639–5648.
32. Frisch MJ, Pople JA, Binkley JS. *J. Chem. Phys.* 1984; **80**: 3265–3269.
33. Cizek J. *Adv. Chem. Phys.* 1969; **14**: 35–89.
34. Purvis GD, Bartlett RJ. *J. Chem. Phys.* 1982; **76**: 1910–1918.
35. Frisch MJ, Trucks GW, Schlegel HB, Scuseria GE, Robb MA, Cheeseman JR, Zakrzewski VG, Montgomery JA Jr, Stratmann RE, Burant JC, Dapprich S, Millam JM, Daniels AD, Kudin KN, Strain MC, Farkas O, Tomasi J, Barone V, Cossi M, Cammi R, Mennucci B, Pomelli C, Adamo C, Clifford S, Ochterski J, Petersson GA, Ayala PY, Cui Q, Morokuma K, Malick DK, Rabuck AD, Raghavachari K, Foresman JB, Cioslowski J, Ortiz JV, Baboul AG, Stefanov BB, Liu G, Liashenko A, Piskorz P, Komaromi I, Gomperts R, Martin RL, Fox DJ, Keith T, Al-Laham MA, Peng CY, Nanayakkara A, Gonzalez C, Challacombe M, Gill PMW, Johnson B, Chen W, Wong MW, Andres JL, Gonzalez C, Head-Gordon M, Replogle ES, Pople JA. *Gaussian 98, Revision A.7*. Gaussian: Pittsburgh, PA, 1998.
36. Geijo F, LopezCalahorra F, Olivella S. *J. Heterocycl. Chem.* 1984; **21**: 1785–1788.
37. Sauers RR. *Tetrahedron Lett.* 1996; **37**: 149–152.
38. Kuhn N, Kratz T. *Synthesis* 1993; 561–562.
39. Schwerdtfeger P, Laakkonen L, Pyykko P. *J. Chem. Phys.* 1992; **96**: 6807–6819.
40. Hoffmann R, Gleiter R, Mallory FB. *J. Am. Chem. Soc.* 1970; **92**: 1460–1466.
41. Arduengo AJ III, Dias HVR, Calabrese JC, Davidson F. *Inorg. Chem.* 1993; **32**: 1541–1542.
42. Cooper WF, Edmonds JW, Wudl F, Coppens P. *Cryst. Struct. Commun.* 1974; **3**: 23.
43. Cetinkaya E, Hitchcock PB, Kucukbay H, Lappert MF, Aljuaid S. *J. Organomet. Chem.* 1994; **481**: 89–95.
44. Cetinkaya E, Hitchcock PB, Jasim HA, Lappert MF, Spyropoulos K. *J. Chem. Soc., Perkin Trans. 1* 1992; 561–567.
45. Anderson DM, Hitchcock PB, Lappert MF. *J. Organomet. Chem.* 1989; **363**: C7–C11.
46. Bourissou D, Guerret O, Gabbai FP, Bertrand G. *Chem. Rev.* 2000; **100**: 39–91.
47. Fekete A, Nyulaszi L. *J. Organomet. Chem.* 2002; **643–644**: 278–284.
48. Arduengo AJ, Dias HVR, Dixon DA, Harlow RL, Klooster WT, Koetzle TF. *J. Am. Chem. Soc.* 1994; **116**: 6812–6822.
49. Jursic BS. *J. Chem. Soc., Perkin Trans. 2* 1999; 1805–1809.
50. Arduengo AJ, Calabrese JC, Davidson F, Dias HVR, Goerlich JR, Krafczyk R, Marshall WJ, Tamm M, Schmutzler R. *Helv. Chim. Acta* 1999; **82**: 2348–2364.
51. Herrmann WA, Kocher C. *Angew. Chem. Int. Ed. Engl.* 1997; **36**: 2163–2187.
52. Arduengo AJ, Gamper SF, Tamm M, Calabrese JC, Davidson F, Craig HA. *J. Am. Chem. Soc.* 1995; **117**: 572–573.
53. Magill AM, Cavell KJ, Yates BF. *J. Am. Chem. Soc.* 2004; **126**(28): 8717–8724.